JOURNAL OF MATERIALS SCIENCE 29 (1994) 721–727

Chemorheology of epoxy resin Part I Epoxy resin cured with tertiary amine

K. C. CHENG, W. Y. CHIU, K. H. HSIEH
Department of Chemical Engineering, National Taiwan University, Taipei, Taiwan, ROC 106
C. C. M. MA
Department of Chemical Engineering, National Tsing Hua University, Hsinchu, Taiwan, ROC 300

Epoxy resin was cured with a tertiary amine. The viscosity and dynamic mechanical properties during the curing reaction were measured by a cone-and-plate rheometer. A dual Arrhenius viscosity model was modified to predict the viscosity profile before gelation during the non-isothermal curing. The viscosity profile coincided with the experimental data. The activation energy of this system calculated using the modified model was 19.8 kcal mol^{-1} for the first region, and 17.3 kcal mol^{-1} for the second region. After gelation, the dynamic complex modulus was related to the reaction kinetics according to the rubber elasticity theory, and the activation energy was 15.3 kcal mol^{-1}. Furthermore, the gelling point can be estimated from the rheological measurements.

1. Introduction

Epoxy resin is one of the most important thermosetting polymers used in many industrial applications, owing to its great versatility, low shrinkage, good chemical resistance, and outstanding adhesion [1]. The end product performance of thermosets is related to not only the composition of reactants but also the processing condition. Monitoring models of rheological properties, viscosity and dynamic moduli, during curing are necessary to be set up for optimal manufacturing operation, such as temperature programmes [2–10].

A series of studies was made during the curing reaction to investigate (1) rheological properties of unmodified epoxy resin, (2) the rheological properties of polyurethane (PU)-cross-linked epoxy resin [11], and comparison with those of the unmodified epoxy resin, and (3) the relationships between the curing conditions and the dynamic properties of fibre-reinforced composites of the PU-cross-linked epoxy resin.

There are several models proposed to correlate with the isothermal viscosity profiles before gelation [12–14]. In particular, a simple model which is used is

$$\ln \eta(t) = \ln \eta_0 + kt \quad (1)$$

where $\eta(t)$ is the viscosity as function of time, t, η_0 is the zero-time viscosity, and k is the apparent kinetic factor. Assuming that η_0 and k can be expressed in Arrhenius form, one can express the isothermal viscosity profile as a function of curing temperature, T, and time

$$\ln \eta(t) = \ln \eta_\infty + \Delta E_\eta / RT + tk_\infty \exp(-\Delta E_k/RT) \quad (2)$$

where $\eta(t)$ is the viscosity as a function of time at a constant temperature, T, and R is the gas constant. There are four parameters in this model: ΔE_η, the activation energy for viscosity; η_∞, Arrhenius pre-exponential viscosity; ΔE_k, the activation energy for reaction, and k_∞, pre-exponential kinetic factor. For the non-isothermal system, the equation was as follows [13]

$$\ln \eta(t, T) = \ln \eta_\infty + \Delta E_\eta / RT(t) + \int_0^t k_\infty \exp[-\Delta E_k/RT(t)]\,dt \quad (3)$$

where the curing temperature, T, is assumed to be a function of the reaction time.

Mussatti and Macosko [15] have proposed a kinetic model to predict the modulus of the reaction mixture after gelation. The thermosetting reaction resin was assumed to exhibit ideal rubber behaviour from the gelation to vitrification. According to the theory of ideal rubber elasticity, the equation can be expressed as

$$|G^*| = RTX \quad (4)$$

where $|G^*|$ is the complex dynamic modulus, T is in an absolute temperature, and X is the cross-link density of the reaction mixture. By an analogy with an nth order irreversible chemical reaction, the rate of the formation of the cross-links can be written as

$$\frac{dX}{dt} = k_x(X_\infty - X)^n \quad (5)$$

where k_x is the kinetic factor of the cross-linking reaction, and X_∞ is the cross-link density after complete curing. The gel time can be estimated to be t_0, at which the tangent line of the rapidly rising portion of the complex modulus curve intersects with the time axis [16]. Assuming the rate of the formation of the cross-links to be a first order reaction, and $|G^*|$ to be

0022–2461

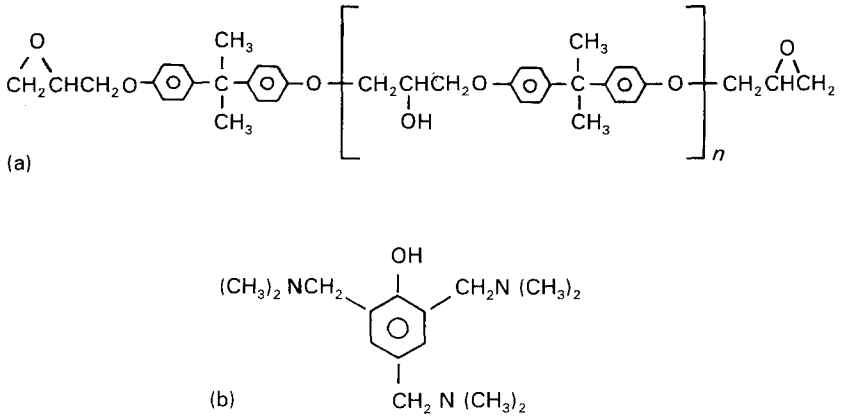

Figure 1 Chemical formula of (a) the epoxy resin (DGEBA) and (b) the tertiary amine catalyst (TDAP).

zero at t_0, the substitution of Equation 4 into Equation 5 yields

$$|G^*| = |G^*_\infty| - |G^*_\infty| \exp[-k_x(t - t_0)] \quad (6)$$

where $|G^*_\infty|$ is the complex modulus near an infinite time. Equation 6 can be rewritten as

$$\ln\left(1 - \frac{|G^*|}{|G^*_\infty|}\right) = k_x(t - t_0) \quad (7)$$

The value of k_x is a function of temperature and can be expressed in Arrhenius form

$$k_x = k_{x\infty} \exp(-\Delta E_x / RT) \quad (8)$$

where ΔE_x is the apparent activation energy for the cross-linking reaction, and $k_{x\infty}$ is the pre-exponential kinetic factor of k_x.

In this study, a cone-and-plate rheometer was applied to monitor the rheological properties of epoxy resin during curing. The viscosity and dynamic modulus profiles were investigated with suitable modification of the above viscosity and modulus models. The gelation times were estimated from the rheological measurements.

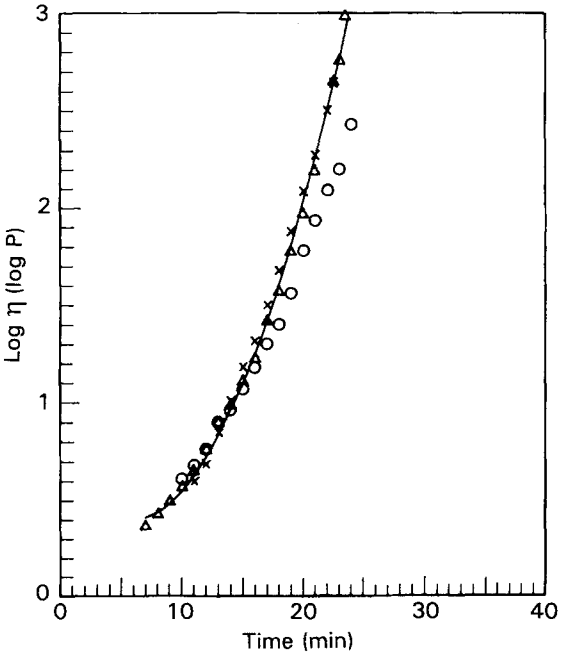

Figure 2 Viscosity versus curing time (at T = 80 °C) at various shear rates (TDAP = 3 p.h.r.). (○) 4 s^{-1}, (×) 2 s^{-1}, (△) 1 s^{-1}. (1 CP = 10^{-3} Ns m^{-2}.)

2. Experimental procedure

2.1. Materials

The epoxy resin used in this study was a diglycidyl ether of bisphenol A with an epoxy equivalent weight 186–192 (Dow Chemical Co.), which was cured with a tertiary amine, 2,4,6-tris(dimethylaminomethyl)phenol (TDAP, Merck Chemical Co.). The chemical formulae are shown in Fig. 1. The epoxy resin was heated and agitated under vacuum for degassing overnight before use.

2.2. Measurements

Rheological measurements were obtained using a rheometer (IR series type, Iwamoto Seisakusho Co. Ltd) with a cone (3° angle) and a plate, 6 cm diameter for shear viscosity measurements, or 3 cm for dynamic modulus tests. The epoxy resin was heated in a beaker to the set temperature, then the curing agent was added to the epoxy resin. After 1–2 min mixing with a stirrer, the reacting sample was poured immediately into the rheometer, which had been heated to the set temperature, and then the sample, cone and plate were enclosed in a chamber temperature-controlled by forced convection (accuracy ± 1 °C). The viscosity profile with time was measured at a constant shear rate, and the resulting stress was recorded. For dynamic properties, the storage modulus, G', and loss modulus, G'', were obtained by applying a sinusoidally varying strain at a fixed frequency and a constant strain amplitude, ± 2°.

3. Results and discussion

3.1. Shear viscosity before the gelling point

The dependency of viscosity profiles on shear rate during the isothermal curing is shown in Fig. 2. In the early stage of curing, the viscosity is independent of shear rate. The viscosity increases with increasing reaction time due to the curing reactions, whereas the viscosity rises sharply and tends to an infinite value as the reaction approaches the gelling point of

the system. Meanwhile, shear thinning behaviour (the viscosity decreases as the shear rate increases) is observed at this region. Measurements of the viscosity profile with time at various curing temperatures are shown in Fig. 3. As the curing temperature increases, the rate of increase in viscosity increases, and the time for the viscosity to approach an infinite value, i.e. t_{η_∞} [17], decreases. The value of t_{η_∞} is suggested to be the time of gelation. It was also found that the higher the content of the curing agent, the higher was the rate of increase of viscosity (Fig. 4). This indicates that the rate of the curing reaction increases with either increasing temperature or the curing agent content.

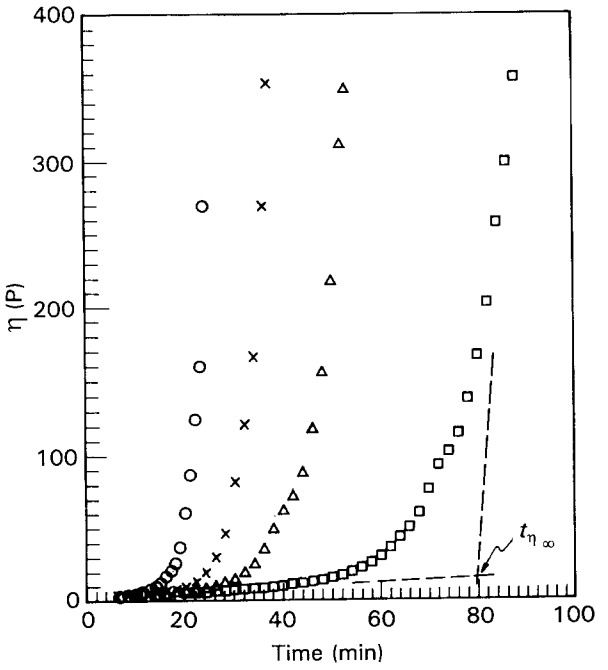

Figure 3 Viscosity versus curing time at various temperatures (at shear rate = 4 s^{-1}, TDAP = 3 p.h.r.). (○) 80 °C, (×) 70 °C, (△) 65 °C, (□) 60 °C.

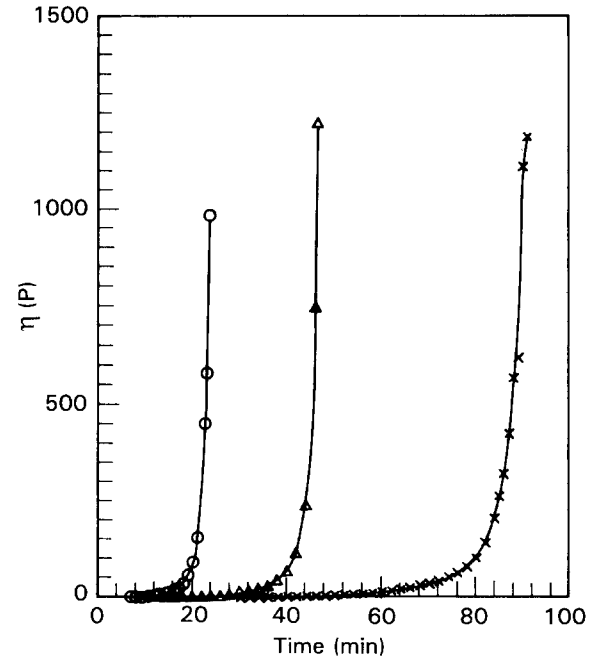

Figure 4 Viscosity versus curing time with various amounts of TDAP (at T = 80 °C, shear rate = 1 s^{-1}). (○) 3 p.h.r., (△) 2 p.h.r., (×) 1.5 p.h.r.

Fig. 5 shows the semi-log plot of the viscosity profiles at various temperatures. An inflexion in the rate was observed before the viscosity reached an infinite value, i.e. a change in the slope, which is assumed by an increase of complex intermolecular actions, such as entanglements, with increasing molecular weight of the epoxy during the reaction. Therefore, Equation 1 was modified as

$$\ln \eta = \ln \eta_0 + k_1 t \quad \text{for} \quad t \leqslant t_c \tag{9}$$

$$\ln \eta = \ln \eta_c + k_2(t - t_c) \quad \text{for} \quad t > t_c \tag{10}$$

where η_0 is the zero-time viscosity, t_c is the curing time at the point of inflexion, η_0 is the viscosity at t_c, and k_1 and k_2 are the apparent kinetic factors for the curing time before and after t_c, respectively. By fitting the data as shown in Fig. 5, the parameters of Equations 9 and 10 were determined and are listed in Table I.

k_1 and k_2 could also be expressed in an Arrhenius form

$$k_1 = k_{1\infty} \exp(-\Delta E_{k_1}/RT) \tag{11}$$

$$k_2 = k_{2\infty} \exp(-\Delta E_{k_2}/RT) \tag{12}$$

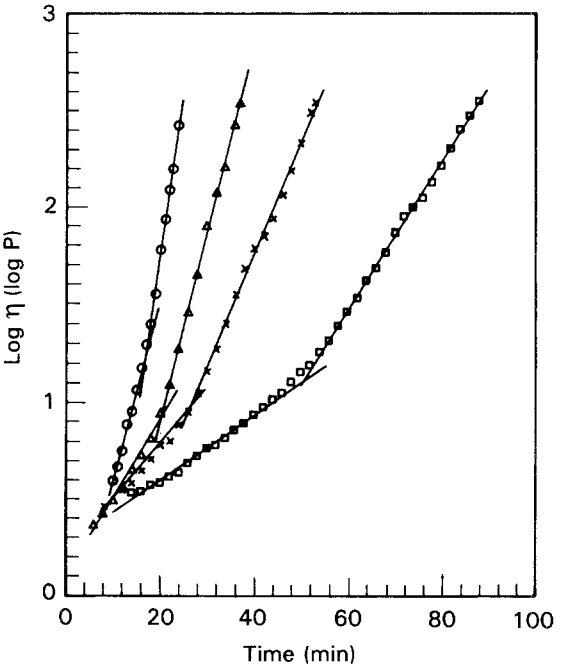

Figure 5 Viscosity versus curing time at various temperatures (at TDAP = 3 p.h.r., shear rate = 4 s^{-1}.) (○) 80 °C, (×) 65 °C, (△) 70 °C, (□) 60 °C.

TABLE I The parameters of Equations 9 and 10 of the modified viscosity model

T(°C)	k_1	k_2	$\ln \eta_0$	$\log \eta_c$	t_c(min)
80	0.216	0.387	−0.81	1.25	17.1
70	0.092	0.221	−0.23	0.92	20.3
65	0.066	0.134	0.48	0.98	26.7
60	0.039	0.088	0.60	1.11	50.6
	$\ln \eta_\infty = -25.1$		$\Delta E_\eta = 17.0$ kcal mol^{-1}		
	$\ln k_{1\infty} = 26.5$		$\Delta E_{k_1} = 19.8$ kcal mol^{-1}		
	$\ln k_{2\infty} = 26.3$		$\Delta E_{k_2} = 17.3$ kcal mol^{-1}		

where ΔE_{k_1} and ΔE_{k_2} are the activation energies of the corresponding reactions for k_1 and k_2, respectively, and $k_{1\infty}$ and $k_{2\infty}$ are the pre-exponential factors. From the Arrhenius plot, as shown in Fig. 6, the apparent activation energies and pre-exponential factors in Equations 11 and 12 were measured from the slopes and intersections of the lines. The values measured are also listed in Table I.

Thus, for the non-isothermal curing reaction, the viscosity profile could also be assumed as a function of curing time, in addition to the temperature, according to the following equation which is analogous to Equation 3

$$\ln \eta(t, T) = \ln \eta_\infty + \Delta E_\eta / RT(t) + \int_0^t k_{1\infty} e^{-\Delta E_{k_1}/RT} dt + \int_{t_c}^t k_{2\infty} e^{-\Delta E_{k_2}/RT} dt \quad (13)$$

Fig. 7 shows the experimental data and calculated values of the temperature–viscosity profiles with the above equation. As the temperature increases from 20 °C to 80 °C, the viscosity initially decreases. However, when the curing reaction progresses, the viscosity decreases to a minimum value and then again increases. This indicates that increasing viscosity may be attributed to the increase in the molecular weight of the reacting epoxy resin. The calculated viscosity profile, as shown in Fig. 7, was obtained from Equation 13 with the two kinetic factors, k_1 and k_2, from Equations 9 and 10, respectively. The predictions of time and the value of the minimum viscosity from Equation 13 are consistent with the experimental data. However, the predicted values are lower than the experimental values as the reaction approaches the gelling point of the reaction.

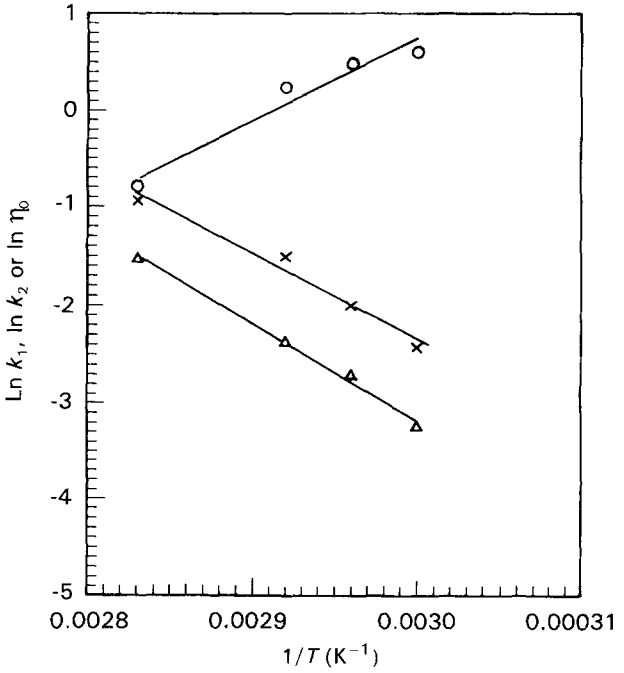

Figure 6 (△) $\ln k_1$, (×) $\ln k_2$ or (○) $\ln \eta_0$ versus $1/T$ (at TDAP = 3 p.h.r., shear rate = 4 s^{-1}).

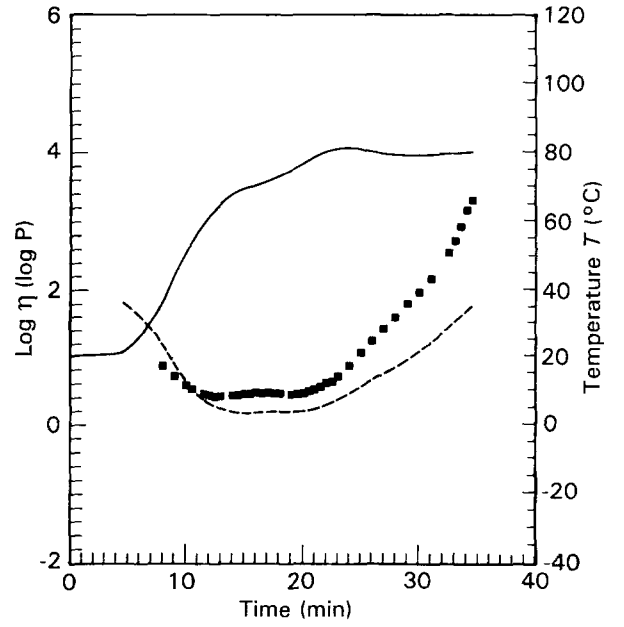

Figure 7 Comparison of (---) the curve of Equation 13 with (■) the measured viscosity (at TDAP = 3 p.h.r., shear rate = 4 s^{-1}, log η_c = 1.0) under non-isothermal conditions. (—) T.

3.2. Dynamic mechanical properties

The dynamic moduli, G' and G'', and loss tangent, tan δ, for the isothermal curing at 80 °C are shown in Fig. 8. In the early stage of curing, the material is still liquid and the molecular weight of the epoxy is low because of the low conversion, so the loss modulus is greater than the storage modulus, and both moduli are very small. Because the elastic property of the resultant mixture increases as the curing reaction progresses, the storage modulus first rises gradually, and then rapidly, eventually exceeding the loss modulus.

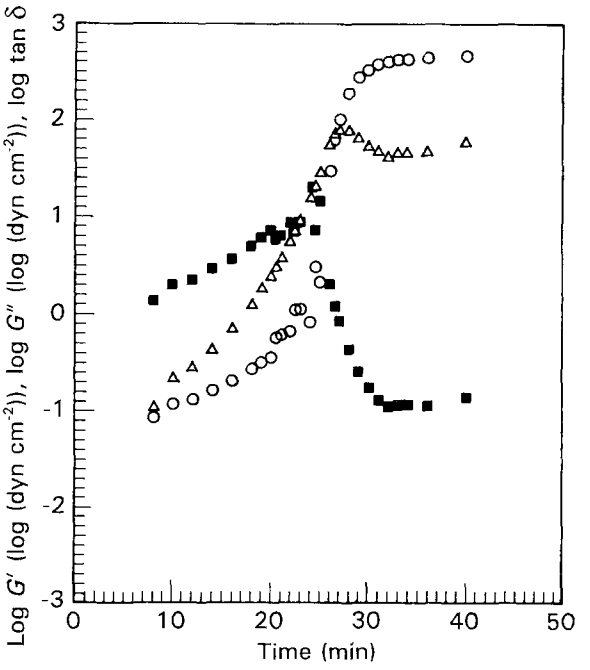

Figure 8 Dynamic mechanical properties versus curing time (at T = 80 °C, TDAP = 3 p.h.r., f = 0.5 Hz.) (○) log G', (△) log G'', (■) log tan δ.

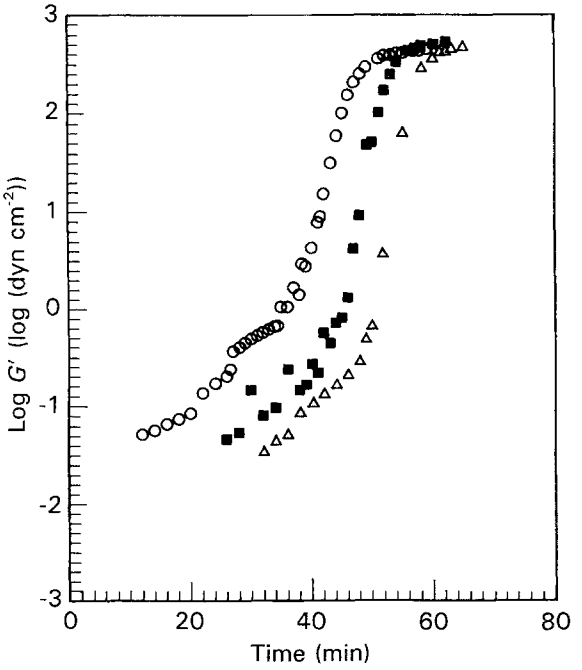

Figure 9 Storage modulus versus curing time at various frequencies (at $T = 70\,°C$, TDAP = 3 p.h.r.). (○) 0.50 Hz, (■) 0.05 Hz, (△) 0.02 Hz.

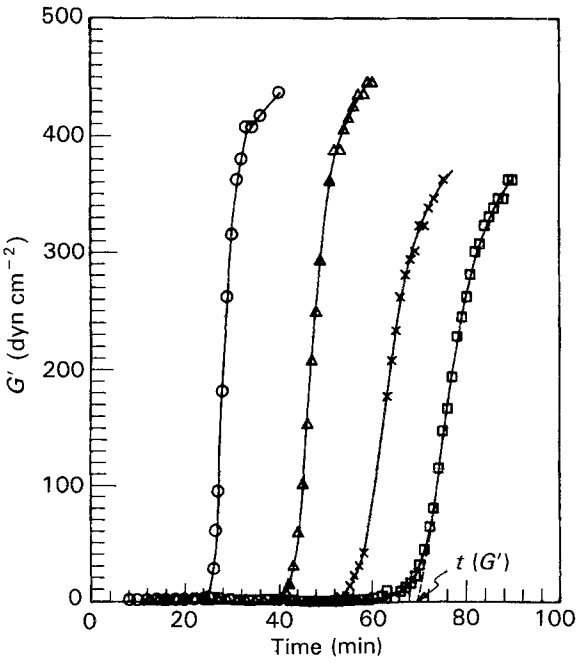

Figure 11 Storage modulus versus curing time at various temperatures (at $f = 0.5$ Hz, TDAP = 3 p.h.r.). (○) 80 °C, (△) 70 °C, (×) 65 °C, (□) 60 °C.

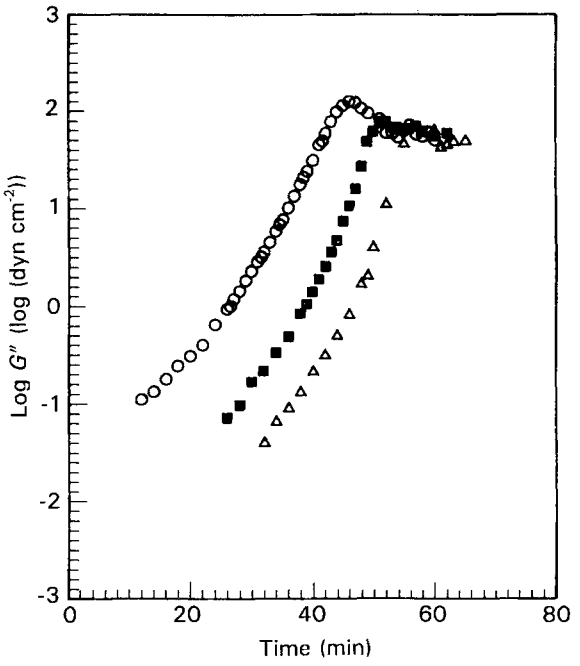

Figure 10 Loss modulus versus curing time at various frequencies (at $T = 70\,°C$, TDAP = 3 p.h.r.). (○) 0.50 Hz, (■) 0.05 Hz, (△) 0.02 Hz.

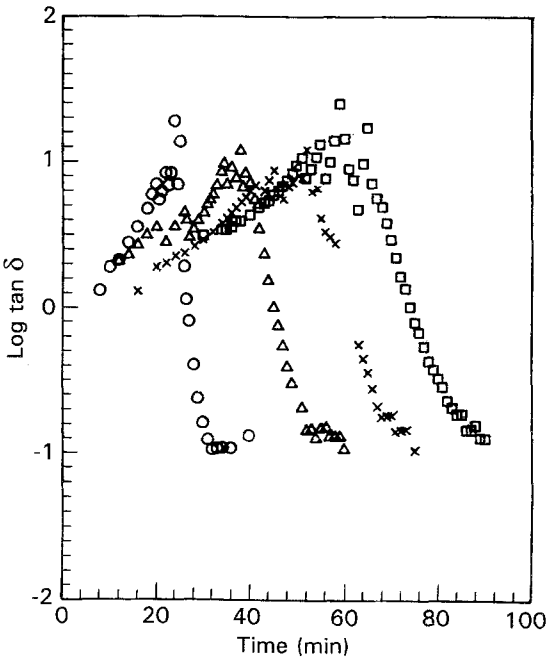

Figure 12 Loss tangent versus curing time at various temperatures (at $f = 0.5$ Hz, TDAP = 3 p.h.r.). (○) 80 °C, (△) 70 °C, (×) 65 °C, (□) 60 °C.

Figs 9 and 10 show the dependency of G' and G'' on frequency, respectively. As the frequency decreases, the curves of G' and G'' tend to shift horizontally from left to right. The dynamic mechanical properties during curing at various temperatures are shown in Figs 11 and 12. The higher curing temperature results in the faster curing reactions, so the time at which G' rises sharply or tan δ reaches a maximum value, is shorter.

The values of t_0, $|G^*_\infty|$ and k_x, in Equations 4–7, were calculated and are listed in Table II. The values of k_x are shown in the Arrhenius plot of Fig. 13. The activation energy, ΔE_x, is 15.3 kcal mol^{-1}, and the value of ln k_x is 20.5. Fig. 14 shows the variation of the calculated values from Equation 6 and the measured values of the complex modulus with time at various temperatures. It is seen that the calculated values agree fairly well with the experimental measurements in the rapidly rising portions of the complex modulus.

3.3. Determination of the gelling time from rheological measurements

There are many different suggestions to determine the gelling time during the isothermal curing from rheological measurements.

1. t_{η_∞}: the gelling time is determined at the intersection point of the two tangent lines of the initial and final portions in the viscosity profile, as seen in Fig. 3. In fact, this time is not the real gelling time, but the rate of increasing viscosity at t_{η_∞} is high enough to suggest that the processing should be completed [12].

2. $t(\tan\delta = 1)$: the time at which the curves of G' and G'' cross each other [18, 19].

3. $t(G''_{max})$: the time to reach maximum loss modulus [20, 21].

4. $t(G')$: the time at which the tangent to the rapidly rising portion of the loss modulus curve intersects the time axis, as shown in Fig. 11 [16].

5. $t(\tan\delta_{max})$: the time at which $\tan\delta$ reaches a maximum value [22].

TABLE II The parameters of dynamic modulus model

T(°C)	t_0(min)	$\lvert G^*_\infty\rvert$ (dyne cm^{-2})	$\ln k_x$
80	26	473	−1.31
70	43	460	−1.56
65	56	453	−2.43
60	68	447	−2.51

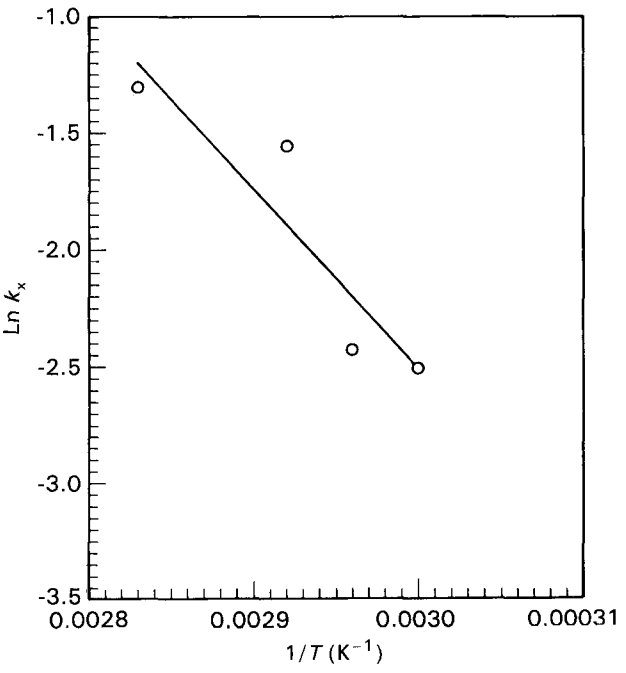

Figure 13 $\ln k_x$ versus $1/T$ for the epoxy reaction (at $f = 0.5$ Hz, TDAP = 3 p.h.r.).

As shown in Table III, the gel times determined from the above dynamic measurements are found to be affected by frequency. However, at high curing temperature (say, at 80 °C), the effect of the gelling times on the frequency is not significant because of the rapid reactions. Furthermore, both values of the $t(G')$ and t_{η_∞} are smaller than those of $t(\tan\delta = 1)$. The value of $t(\tan\delta = 1)$ is almost the same as $t(G''_{max})$. It was also found that the value of $t(\tan\delta_{max})$ is closer to t_{η_∞} than the other values.

4. Conclusion

The viscosity and complex dynamic modulus of the epoxy system cured with the tertiary amine (TDAP) under isothermal and non-isothermal conditions, were studied. A modified viscosity model from the dual Arrhenius model was proposed to predict the viscosity profile before gelation. For the isothermal curing, the calculated complex modulus on the basis of the rubber elasticity theory agrees fairly well with the experimental measurements after the gelling point of the reaction. Furthermore, it was found that the time at which $\tan\delta$ reaches a maximum value almost

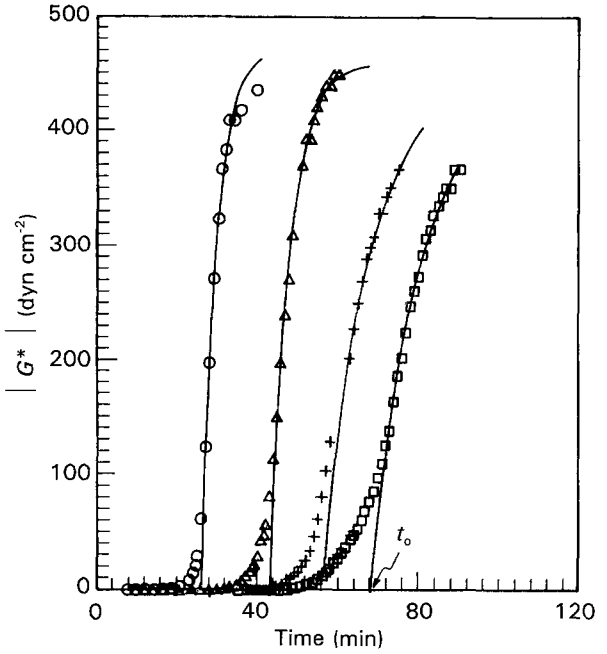

Figure 14 Comparison of the curve of Equation 6 with the measured complex modulus (at TDAP = 3 p.h.r., $f = 0.5$ Hz). (○) 80 °C, (△) 70 °C, (+) 65 °C, (□) 60 °C.

TABLE III The gelling times determined from rheological measurements

T (°C)	Frequency (Hz)	$t(\tan\delta = 1)$ (min)	$t(G''\text{max})$ (min)	$t(G')$ (min)	$t(\tan\delta_{max})$ (min)	t_{η_∞} (min)	$\dot\gamma^a$ (s^{-1})
80	0.5	27	27	26	24	21	1
80	0.1	27	27	27	25	21	2
80	0.05	27	27	27	23	21.5	4
70	0.5	44	44	42	37	33	1
70	0.05	50	50	48	44	29	2
70	0.02	54	54	54	50	34	4
65	0.5	60	62	56	52	48	4
60	0.5	75	75	70	65	79	4

[a] $\dot\gamma$, shear rate.

coincides with the time at which the shear viscosity approaches an infinite value.

Acknowledgement

We thank the National Science Council, Taipei, Taiwan, ROC, for financial support of this study under contract NSC 79-040S-E-002-10.

References

1. C. A. MAY, in "Epoxy Resins–Chemistry and Technology" edited by C. A. May (Dekker, New York, 1988) p. 1.
2. L. NICOLAIS and A. APICELLA, *Pure Appl. Chem.* **57** (1985) 1701.
3. G. A. SENICH, W. J. MacKNIGHT and N. S. SCHNEIDER, *Polym. Eng. Sci.* **19** (1979) 313.
4. C. Y. YAP and H. L. WILLIAMS, *ibid.* **22** (1982) 254.
5. M. ADAM, M. DELSANTI and D. DURAND, *Macromolecules* **18** (1985) 2285.
6. N. S. SCHNEIDER, J. F. SPROUSE, G. L. HAGNAUER and J. K. GILLHAM, *Polym. Eng. Sci.* **19** (1979) 304.
7. F. CHAMBON, Z. S. PETROVIC, W. J. MACKNIGHT and H. H. WINTER, *Macromolecules* **19** (1986) 2146.
8. B. Z. JANG and G. H. ZHU, *J. Appl. Polym. Sci.* **31** (1986) 2627.
9. W. X. ZUKAS, *Polym. Eng. Sci.* **29** (1989) 1553.
10. M. S. HEISE and G. C. MARTIN, *ibid.* **30** (1990) 83.
11. J. L. HAN, S. M. TSENG, J. H. MAI and K. H. HSIEH, *Angew. Makromol. Chem.* **182** (1990) 193.
12. R. P. WHITE Jr, *Polym. Eng. Sci.* **14** (1974) 50.
13. M. B. ROLLER, *ibid.* **15** (1975) 406.
14. *Idem, ibid.* **26** (1986) 432.
15. F. G. MUSSATTI and C. W. MACOSKO, *ibid.* **13** (1973) 236.
16. P. E. WILLARD, *ibid.* **14** (1974) 273.
17. C. D. HAN and K. W. LEM, *J. Appl. Polym. Sci.* **28** (1983) 3155.
18. C. M. TUNG and P. J. DYNES, *ibid.* **27** (1982) 569.
19. H. H. WINTER, *Polym. Eng. Sci.* **21** (1987) 1698.
20. J. K. GILLHAM, *ibid.* **19** (1979) 319.
21. *Idem, ibid.* **19** (1979) 676.
22. A. Y. MALKIN and S. G. KULICHIKHIN, *Adv. Polym. Sci.* **101** (1991) 217.

Received 9 September 1992
and accepted 26 August 1993